

## Structure and Function in Rhodopsin: Effects of Disulfide Cross-Links in the Cytoplasmic Face of Rhodopsin on Transducin Activation and Phosphorylation by Rhodopsin Kinase<sup>†,‡</sup>

Kewen Cai,<sup>§</sup> Judith Klein-Seetharaman,<sup>§</sup> John Hwa,<sup>§</sup> Wayne L. Hubbell,<sup>||</sup> and H. Gobind Khorana<sup>\*,§</sup>

*Departments of Biology and Chemistry, Massachusetts Institute of Technology, Cambridge, Massachusetts 02139, and Jules Stein Eye Institute and Department of Chemistry and Biochemistry, University of California, Los Angeles, California 90095*

*Received June 1, 1999; Revised Manuscript Received July 29, 1999*

**ABSTRACT:** Six rhodopsin mutants containing disulfide cross-links between different cytoplasmic regions were prepared: disulfide bond 1, between Cys65 (interhelical loop I–II) and Cys316 (end of helix VII); disulfide bond 2, between Cys246 (end of helix VI) and Cys312 (end of helix VII); disulfide bond 3, between Cys139 (end of helix III) and Cys248 (end of helix VI); disulfide bond 4, between Cys139 (end of helix III) and Cys250 (end of helix VI); disulfide bond 5, between Cys135 (end of helix III) and Cys250 (end of helix VI); and disulfide bond 6, between Cys245 (end of helix VI) and Cys338 (C-terminus). The effects of local restrictions caused by the cross-links on transducin ( $G_T$ ) activation and phosphorylation by rhodopsin kinase (RK) following illumination were studied. Disulfide bond 1 showed little effect on either  $G_T$  activation or phosphorylation by RK, suggesting that the relative motion between interhelical loop I–II and helix VII is not crucial for recognition by  $G_T$  or by RK. In contrast, disulfide bonds 2–5 abolished both  $G_T$  activation and phosphorylation by RK. Disulfide bond 6 resulted in enhanced  $G_T$  activation but abolished phosphorylation by RK, suggesting the structure recognized by  $G_T$  was stabilized in this mutant by cross-linking of the C-terminus to the cytoplasmic end of helix VI. Thus, the consequences of the disulfide cross-links depended on the location of the restriction. In particular, relative motions of helix VI, with respect to both helices III and VII upon light activation, are required for recognition of rhodopsin by both  $G_T$  and RK. Further, the conformational changes in the cytoplasmic face that are necessary for protein–protein interactions need not be cooperative, and may be segmental.

Light initiates two biochemical cascades in rhodopsin, one leading to sensitization (amplification) and the other to desensitization (quenching). Binding and activation of  $G_T$ <sup>1</sup> and of RK are, respectively, the first events in the two cascades. Competition between  $G_T$  and RK for occupancy of the light-activated rhodopsin and its phosphorylated form must be central to the progression of the two cascades. Therefore, understanding the requirements of the two proteins for binding to rhodopsin is of interest. Ideally, three-dimensional structures of the complexes of the two proteins with rhodopsin are needed, but such structural analysis lies in the future. Alternative biochemical approaches have

provided some insights into the sites involved in binding of the two proteins to rhodopsin. Thus, inhibition of  $G_T$  activation by peptides corresponding to the amino acid sequences in the different cytoplasmic loops (2) and mutagenic studies (3) have indicated that a considerable portion of the cytoplasmic face of light-activated rhodopsin is involved in binding to  $G_T$ . Furthermore, mutagenic studies on the binding of RK to rhodopsin also indicate that at least the amino acid loop sequences connecting TM helices III and IV, and helices V and VI (Figure 1), are involved (4–6).

Here we report on an alternative approach to the study of requirements for  $G_T$  activation and phosphorylation of rhodopsin by RK that involves placing local restrictions on the conformational change in light-activated rhodopsin. In previous studies, helix movements in the TM domain were demonstrated on photoactivation of rhodopsin by EPR spectroscopy of spin-labeled cysteine residues in the cytoplasmic domain (7–12). Further, disulfide cross-links between cysteines placed in the cytoplasmic loops at the ends of helices III and VI were shown to block  $G_T$  activation, presumably due to local restriction of the conformational change (9). A similar result was reported as a consequence of mutagenic insertion of histidine residues in the cytoplasmic face followed by their chelation through a zinc ion (13). More recently, in the mapping of proximity relationships between different amino acids in the presumed tertiary structure in the cytoplasmic face, spontaneous disulfide bond formation

<sup>†</sup> This work was supported by NIH Grants GM28289 and NEI EY11716 (H.G.K.) and NIH Grant EY05216 and the Jules Stein Professorship Endowment (W.L.H.). J.K.-S. is the recipient of a Howard Hughes Medical Institute Predoctoral Fellowship. J.H. is the recipient of a Howard Hughes Medical Institute Physician Postdoctoral Fellowship.

<sup>‡</sup> This is paper 36 in the series “Structure and Function in Rhodopsin”. The preceding paper is by Hwa et al. (1).

\* To whom correspondence should be addressed.

<sup>§</sup> Massachusetts Institute of Technology.

<sup>||</sup> University of California.

<sup>1</sup> Abbreviations:  $G_T$ , transducin; RK, rhodopsin kinase; 4-PDS, 4,4'-dithiodipyridine; DM, dodecyl maltoside; DTT, dithiothreitol; Meta II, metarhodopsin II; TM, transmembrane; WT, wild-type;  $A_{280}$  or  $A_{500}$ , absorbance at 280 or 500 nm; EPR, electron paramagnetic resonance. Opsin mutants with amino acid replacements are designated by one-letter abbreviations for amino acids; the letter to the left of the residue number is the original, whereas that to the right is the amino acid to which the residue is being changed.

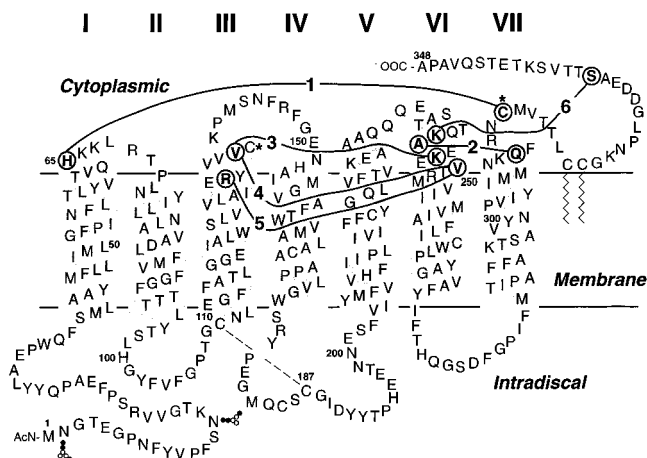


FIGURE 1: Disulfide cross-links, numbered 1–6, between cysteines at circled positions shown in a secondary structure model of rhodopsin. In all the cysteine substitutions, the two reactive native cysteines, Cys140 and Cys316, denoted by asterisks were replaced with serine residues except for disulfide cross-link 1 which involved Cys316 as one of the two cysteines.

Table 1: Sets of Cysteine Pairs Studied for Proximity Relationships in the Tertiary Structure of the Cytoplasmic Face of Rhodopsin

cysteine pairs		disulfide bonds formed most rapidly	disulfide bond number (Figure 1)
cysteine 1 (fixed)	cysteine 2 (varied)		
Cys65	Cys306 to Cys321	Cys65–Cys316 <sup>a</sup>	1
Cys316	Cys60 to Cys74	Cys65–Cys316 <sup>a</sup>	1
Cys246 or Cys250	Cys311 to Cys314	Cys246–Cys312 <sup>a</sup>	2
Cys139	Cys247 to Cys252	Cys139–Cys248 <sup>b</sup>	3
		Cys139–Cys250 <sup>b</sup>	4
Cys135	Cys250	Cys135–Cys250 <sup>a</sup>	5
Cys338	Cys240 to Cys250	Cys245–Cys338 <sup>c</sup>	6

<sup>a</sup> Unpublished data of Cai et al. and Klein-Seetharaman et al. <sup>b</sup> See ref 9. On the basis of EPR studies, these two cysteine pairs exhibited the strongest spin–spin interactions. <sup>c</sup> See ref 14.

between cysteine pairs in different locations has been studied systematically (refs 10 and 14 and unpublished data of Cai et al. and Klein-Seetharaman et al.). Six sets of double-cysteine mutants shown in Table 1 were studied. In each set, cysteine pairs that formed the disulfide bond most rapidly or participated in the strongest interactions between spin-labels attached to the cysteines were identified (Table 1 and Figure 1). The disulfide-bonded products formed from these cysteine pairs have now been studied for their effects on the binding and activation of G<sub>T</sub> and RK following light activation.

Such disulfide bonds individually would be expected to cause local restrictions of the conformational change, and the effects on activation of the two proteins may exhibit distinctive features. The effects of disulfide bonds 1–6 (Figure 1) experimentally found and documented here fall into three groups. Disulfide bond 1, between Cys65 and Cys316, has no significant effect on either G<sub>T</sub> activation or phosphorylation by RK. Disulfide bond 2, between Cys246 and Cys312, and disulfide bonds 3–5, between Cys139 and Cys248, between Cys139 and Cys250, and between Cys135 and Cys250, respectively, all abolished both G<sub>T</sub> activation and phosphorylation by RK. Finally, disulfide bond 6, between Cys245 at the end of helix VI and Cys338 in the C-terminus (Figure 1), in fact, enhanced G<sub>T</sub> activation but

abolished, as might have been expected, phosphorylation by RK. Overall, the results show that the light-induced structural changes in the cytoplasmic face that are required for interaction with G<sub>T</sub> and RK need not be cooperative and global but, instead, may be segmental.

## MATERIALS AND METHODS

Unless stated otherwise, these were as described previously (14, 15). Nitrocellulose membranes were obtained from Schleicher & Schuell. [ $\gamma$ -<sup>32</sup>P]ATP (3000 Ci/mmol, 1 Ci/37 GBq) was from DuPont/NEN. G<sub>T</sub> was purified from bovine rod outer segments as described by Baehr et al. (16). RK, purified from baculovirus-infected Sf21 cells, was kindly provided by K. Cha of this laboratory (17).

*Construction of Plasmids Containing Single- and Double-Cysteine Codons in the Bovine Opsin Gene.* Construction of plasmids containing cysteine mutations, Q312C, S338C, and H65C, and the mutant containing the single native cytoplasmic cysteine C316 has been described previously (14, 15, 18, 19). A two-step PCR mutagenesis technique (14) was used for introducing the mutation, R135C. Starting with the parent plasmid containing mutations C140S and C316S, PCR was performed with the following primer and its complement, 5'GGCGATCGAGTGCTACGTGGTGG3'. The PCR product was digested to yield a *Xho*I–*Nhe*I fragment containing the R135C substitution. This fragment was then subcloned into the parent plasmid.

For preparation of single-cysteine mutants K248C and T250C, previously prepared plasmids (20) were digested with *Mlu*I–*Not*I to excise the small fragments containing the C322S and C323S substitutions. The large fragments thus generated were ligated to the small *Mlu*I–*Not*I fragments from the C140S/C316S plasmid described above that contained the palmitoylation sites C322 and C323. For preparation of the single-cysteine mutant V139C, the plasmid (plasmid A) containing the substitutions C322S, C323S, C167S, C222S, and C264S (21) and the plasmid containing only substitutions C140S and C316S described above (now designated plasmid B) were digested with *Eco*RI–*Pst*I. The small fragment obtained from both constructs was further digested with *Bsa*HI. The *Eco*RI–*Bsa*HI fragment now obtained from the plasmid A was ligated, in a three-part ligation, with the small *Bsa*HI–*Pst*I fragment and the large *Eco*RI–*Pst*I fragment from plasmid B.

Construction of the plasmids containing cysteine pairs, K245C/S338C and H65C/C316S, have been described previously (10, 14). For the double-cysteine mutant R135C/V250C, the PCR product described above in the preparation of the mutant R135C was now digested with *Xho*I–*Pst*I and the small fragment obtained was ligated in a three-part ligation with the *Pst*I–*Bsp*EI fragment from the mutant V250C/S338C plasmid (14) and the large *Xho*I–*Bsp*EI fragment from the parent C140S/C316S plasmid.

The mutants V139C/K248C and V139C/T250C were prepared from the previously prepared corresponding plasmids that lacked the palmitoylation sites (9). The plasmids were digested with *Eco*RI and *Nde*I, and the *Eco*RI–*Nde*I fragment (nucleotides 1061–1867) was purified. The base mutant C140S/C316S plasmid was first digested with *Eco*RI–*Nhe*I. The resulting small fragment was further cut by *Nde*I. The *Nde*I–*Nhe*I fragment was ligated with the large

*EcoRI*–*NheI* fragment from plasmid C140S/C316S, followed by ligation of the resulting ligated product with the *EcoRI*–*NdeI* fragment from the mutant plasmid containing V139C/K248C or V139C/V250C replacements. Mutant A246C/Q312C was prepared from the plasmid containing the single-cysteine substitution Q312C (15). The *MluI*–*NheI* restriction fragment in plasmid A246C/S338C was replaced with the *MluI*–*NheI* fragment from Q312C.

*Isolation of Double-Cysteine Mutants in Reduced and Oxidized Forms.* Expression in COS-1 cells and purification of the mutants were as described previously (14). To obtain the expressed mutants in the sulfhydryl forms, elution from 1D4-Sepharose was carried out at pH 6 under argon. For oxidation to the disulfide-bonded forms, the pH of the solubilized mutants was raised above 7.5. Rates of disulfide bond formation in different sets of mutants have been described elsewhere (ref 14 and unpublished data of Cai et al. and Klein-Seetharaman et al.). Completion of the formation of the disulfide bonds was confirmed in every case by testing with 4-PDS as described previously (14).

*Retinal Chromophore Isomer Composition Analysis in Light-Activated Rhodopsin Mutants.* Retinal was extracted from 200  $\mu$ L of 1.5  $\mu$ M rhodopsin immediately after illumination (30 s). Samples were first treated with 500  $\mu$ L of ice-cold ethanol by vortexing for 2 min, and were then mixed with 500  $\mu$ L of ice-cold hexane by vortexing for an additional 2 min (22). Aliquots (450  $\mu$ L) of the hexane phase were immediately analyzed by HPLC (Rainin SD-200) using a DuPont Zorbex-sil column (4.6 mm  $\times$  250 mm). The different isomers were separated using the solvent system, 92% hexane and 8% diethyl ether. Elution was carried out at a flow rate of 0.5 mL/min, and the effluent was monitored by  $A_{380}$ .

*Determination of G<sub>T</sub> Activation Rates.* Activation of G<sub>T</sub> by rhodopsin was monitored using fluorescence spectroscopy (PTI fluorometer) at 20 °C as described previously (15). The excitation wavelength was 295 nm with a 2 nm slit width, and the emission wavelength was 340 nm with a 12 nm slit width. G<sub>T</sub> was added (final concentration of 250 nM) to the reaction mixture containing 10 mM Tris (pH 7.2), 2 mM MgCl<sub>2</sub>, 100 mM NaCl, and 0.012% DM. The solution was stirred for 300 s to establish a baseline. Photobleached rhodopsin was then added to the mixture to a final concentration of 5 nM. Photobleaching was carried out using >495 nm light for 10 s. After an additional 600 s, GTP $\gamma$ S was added to the reaction mixture to a final concentration of 5  $\mu$ M, and the increase in fluorescence was followed for an additional 2000 s. To calculate the activation rates, the slopes of the initial fluorescence increase after GTP $\gamma$ S addition were determined by linear regression through the data points covering the first 60 s.

*Determination of Phosphorylation Initial Rates of Rhodopsin Mutants.* The reaction mixture contained 20 mM bis-tris-propane (BTP) (pH 7.5), 2 mM MgCl<sub>2</sub>, 0.03% DM, 30  $\mu$ M [ $\gamma$ -<sup>32</sup>P]ATP (~2000 cpm/pmol), 1.5  $\mu$ M rhodopsin, and about 0.8 unit of RK (1 unit is defined as 1 nmol of phosphates transferred per minute at a rhodopsin concentration of 20  $\mu$ M). The reaction was initiated by illumination. At defined time intervals, aliquots (26  $\mu$ L) of the reaction mixture were diluted with 100  $\mu$ L of stop solution (800 mM KH<sub>2</sub>PO<sub>4</sub> and 20 mM ATP). Samples were then applied to nitrocellulose membranes using a micro-dot blot system (Bio-

Table 2: Characterization of Single- and Double-Cysteine Substitution Mutants

mutant	$\lambda_{\max}$ (nm)	$A_{280}/A_{500}$	Meta II decay $t_{1/2}$ (min)	
			without DTT	with DTT
(A) Single-Cysteine Mutants				
WT	500	1.6	12.2	
C140S/C316S		1.7	13.3	
H65C		1.6	13.4	
R135C		1.8	12.0	
V139C		1.6	15.3	
K245C		1.7	10.8	
A246C		1.6	13.0	
K248C		1.7	12.2	
V250C		1.6	13.3	
Q312C		1.9	12.4	
C316S		1.6	12.3	
S338C		1.6	13.3	
(B) Double-Cysteine Mutants				
mutant	$\lambda_{\max}$ (nm)	$A_{280}/A_{500}$	without DTT	with DTT
WT	500	1.6	13.6	14.7
H65C/C316S	501	1.6	9.8	14.9
A246C/Q312C	500	1.7	7.9	16.1
V139C/K248C	495	1.7	22.6	25.2
V139C/V250C	500	1.7	11.5	13.1
R135C/V250C	500	1.9	8.9	9.8
K245C/S338C	500	1.6	10.3	14.5

Rad). The membranes were washed extensively with 1 M KH<sub>2</sub>PO<sub>4</sub>, and the radioactivity was measured by Cerenkov counting.

For assays carried out in the presence of DTT, rhodopsin samples were preincubated with 1 mM DTT for 1 h at room temperature prior to the assay. Furthermore, the reaction mixtures also contained 1 mM DTT.

## RESULTS

### Characterization of Cysteine Mutants

The yields of the mutants on expression in COS-1 cells were comparable to that of WT rhodopsin.

*Spectral Characterization.* All the single- and double-cysteine mutants formed a WT-like chromophore with  $A_{280}/A_{500}$  ratios between 1.6 and 1.9 (Table 2). Their  $\lambda_{\max}$  in the visible range was close to 500 nm, except mutant V139C/K248C which was 495 nm (Table 2).

*Rates of Meta II Decay in Single- and Double-Cysteine Mutants in Reduced and Disulfide-Bonded Forms.* On illumination, all the single-cysteine mutants formed Meta II which decayed at rates similar to that of WT rhodopsin (Table 2A). All the double-cysteine mutants also formed Meta II ( $\lambda_{380}$ ) normally. The rates of their decay were measured both in the presence and in the absence of DTT. The results are shown in Table 2B. As seen, mutants V139C/K248C, V139C/V250C, and R135C/V250C exhibited similar rates of Meta II decay in reduced and oxidized forms, whereas mutants A246C/Q312C, K245C/S338C, and H65C/C316 exhibited marked differences in the two states. Further, mutants V139C/K248C and R135C/V250C exhibited striking differences with respect to WT rhodopsin in their decay rates.

*Formation of all-trans-Retinal on Illumination of Disulfide-Bonded Mutants.* The effects of cross-links between different regions of the cytoplasmic domain on the nature of retinal isomers formed on illumination were examined. The com-

Table 3: Rates of G<sub>T</sub> Activation and Phosphorylation by RK of the Single-Cysteine Mutants

	relative rate of G <sub>T</sub> activation <sup>a,b</sup>	relative rate of phosphorylation by RK <sup>a,c</sup>
WT	1.0	1.0
C140S/C316S	0.95 ± 0.01	0.84 ± 0.09
H65C	0.75 ± 0.13	0.61 ± 0.07
R135C	0.03 ± 0.01	1.11 ± 0.12
V139C	0.52 ± 0.09	0.41 ± 0.02
K245C	0.71 ± 0.03	0.78 ± 0.10
A246C	0.80 ± 0.09	0.76 ± 0.04
K248C	0.46 ± 0.10	0.45 ± 0.01
V250C	0.58 ± 0.08	0.79 ± 0.03
Q312C	0.88 ± 0.14	0.79 ± 0.07
C316S	0.89 ± 0.15	0.70 ± 0.08
S338C	0.94 ± 0.08	0.83 ± 0.09

<sup>a</sup> Each value of the initial rates was the average of at least three measurements. The error given is the standard deviation. <sup>b</sup> The relative initial rate of G<sub>T</sub> activation is represented by the rate of fluorescence increase relative to that of WT rhodopsin. <sup>c</sup> The relative rate of phosphorylation is represented by the rate of the incorporation of <sup>32</sup>P relative to that of WT rhodopsin.

positions of the retinal isomers after light activation of all six mutants were analyzed by HPLC (Materials and Methods). In all cases, *all-trans*-retinal accounted for more than 94% and *13-cis*-retinal accounted for less than 5%. Because of relatively insignificant differences, the data are not shown.

#### G<sub>T</sub> Activation and Phosphorylation by RK in Single-Cysteine Mutants

As controls for the effect of motion restrictions imposed by the disulfide bonds, all the corresponding single-cysteine mutants were studied for G<sub>T</sub> activation and phosphorylation by RK. While G<sub>T</sub> activation for most of the single-cysteine mutants has been described previously, however, these mutants that had been previously studied lacked the palmitoylation sites (20, 21). In both the double- and single-cysteine mutants that are being studied here, the palmitoylation sites are retained (Materials and Methods).

The results of measurements of the extent of G<sub>T</sub> activation and rates of phosphorylation by RK for the single-cysteine mutants and the base mutant C140S/C316S, from which all the single-cysteine mutants were derived, are summarized in Table 3. Mutants H65C, K245C, A246C, Q312C, C316, and S338C exhibited somewhat decreased activities with respect to both G<sub>T</sub> activation and phosphorylation by RK. However, more significant decreases in the extent of G<sub>T</sub> activation and the rate of phosphorylation were observed in mutants V139C and K248C. Mutant V250C exhibited a 40% decrease in the extent of G<sub>T</sub> activation and a 20% decrease in the rate of phosphorylation by RK. The activation of G<sub>T</sub> was completely abolished in the mutant R135C, while its phosphorylation by RK was essentially WT-like.

#### Disulfide Bond 1 in Rhodopsin (Figure 1) Allows both G<sub>T</sub> Activation and Phosphorylation by RK

Mutant H65C/C316 exhibited essentially no significant difference in G<sub>T</sub> activation in the disulfide-bonded and reduced states (Figure 2A), 60–70% of WT activity (Figure 5). Further, similar phosphorylation rates in disulfide-bonded and reduced states were observed (Figure 2B). The rates were

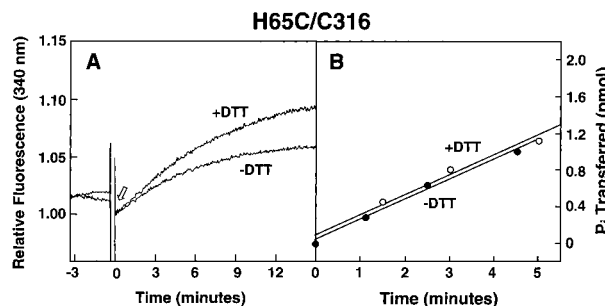


FIGURE 2: Kinetics of G<sub>T</sub> activation and phosphorylation by RK in the disulfide cross-linked mutant H65C/C316 (Figure 1). (A) G<sub>T</sub> activation. GTPγS was added at the time indicated by the arrow. (B) Kinetics of [<sup>32</sup>P]P<sub>i</sub> (picomoles) incorporation into rhodopsin as a function of time. For details, see Materials and Methods.

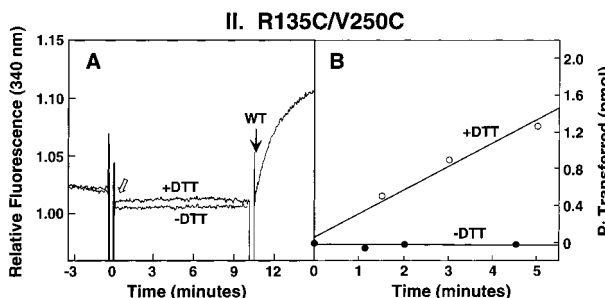
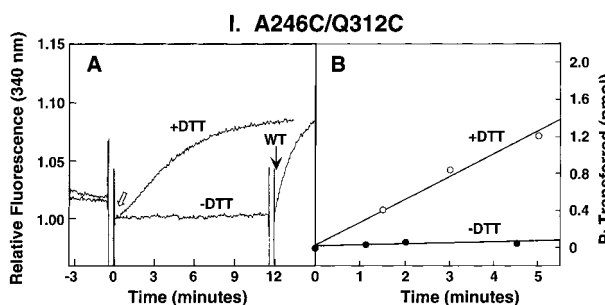


FIGURE 3: G<sub>T</sub> activation and phosphorylation by RK in cross-linked mutants A246C/Q312C (I) and R135C/V250C (II). (A) G<sub>T</sub> activation. GTPγS was added as indicated by the open arrows. In the reaction carried out in the absence of DTT, where no increase in fluorescence was observed, WT rhodopsin was added as an internal control at the times shown by solid arrows. (B) Kinetics of [<sup>32</sup>P]P<sub>i</sub> (picomoles) transfer as a function of time.

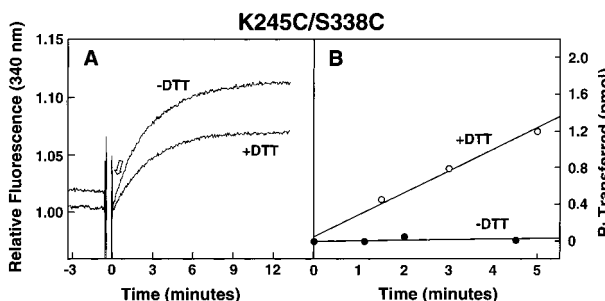


FIGURE 4: Kinetics of G<sub>T</sub> activation and phosphorylation by RK in the cross-linked mutant K245C/S338C. (A) G<sub>T</sub> activation. The arrow indicates the time of GTPγS addition. (B) Kinetics of phosphorylation by RK.

about 50% of that of WT rhodopsin (Figure 5). The decreased activity observed in both G<sub>T</sub> activation and phosphorylation compared to that of WT rhodopsin can likely be ascribed to the effect from the single-cysteine replacement H65C (Table 3).

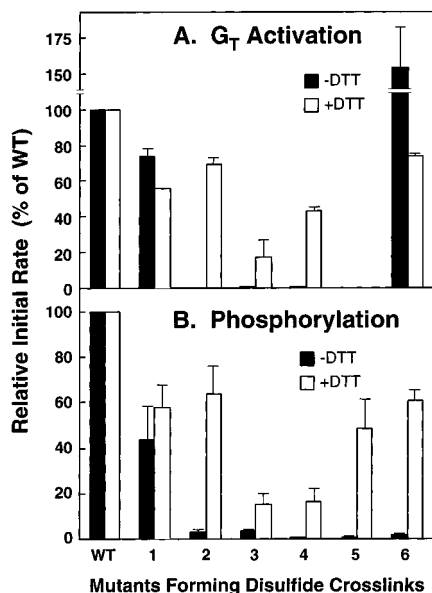


FIGURE 5: Relative initial rates of G<sub>T</sub> activation (A) and phosphorylation by RK (B) for the six mutants in their disulfide-bonded form (-DTT) and in the reduced form (+DTT). The numbers on the x axis correspond to the numbers for cross-links shown in Figure 1 and Table 1.

*Disulfide Bonds 2–5 in Rhodopsin (Figure 1) Abolish both G<sub>T</sub> Activation and Phosphorylation by RK*

Disulfide cross-links in four of the mutants, A246C/Q312C, V139C/K248C, V139C/V250C, and R135C/V250C, all exhibited similar consequences on both G<sub>T</sub> activation and phosphorylation. Therefore, only the data for two of the mutants, A246C/Q312C and R135C/V250C, are depicted in Figure 3. As seen in panels I-A and II-A, G<sub>T</sub> activation was completely abolished in the mutants in their disulfide-bonded states, but was partially restored in three mutants in the presence of DTT except for mutant R135C/V250C (panel II-A, Figure 3). Single-cysteine mutation R135C alone abolished G<sub>T</sub> activation (Table 3). The rates were about 70% of the WT rate for A246C/Q312C and 20–40% of the WT rate for V139C/K248C and V139C/V250C (Figure 5). The variations in activity in the presence of DTT can probably be explained by the additive effects of the single-cysteine replacements (Table 3).

The effects of the four disulfide cross-links described above on phosphorylation by RK were also similar. Thus, in the disulfide-bonded states, phosphorylation was completely abolished in all four mutants (panels I-B and II-B in Figure 3). In the presence of DTT, phosphorylation was recovered partially in all four cases (panels I-B and II-B in Figure 3). The observed reduced rates of phosphorylation in the mutants after DTT treatment, compared to that of WT rhodopsin, likely resulted from the additive effects of the individual cysteine substitutions in each mutant (Table 3).

*Disulfide Bond 6 (Figure 1) Enhances G<sub>T</sub> Activation but Abolishes Phosphorylation by RK*

Disulfide bond 6 substantially enhanced the rate of G<sub>T</sub> activation, 150% of that of WT rhodopsin. The rate of G<sub>T</sub> activation in the presence of DTT was about 70% of that of WT rhodopsin (Figure 4A). However, as might have been expected, this cross-link between the C-terminal tail and the

cytoplasmic end of helix VI abolished phosphorylation (Figure 4B), but the activity was regained in the presence of DTT.

## DISCUSSION

Light activation of rhodopsin is believed to cause a conformational change in the cytoplasmic face of rhodopsin which allows subsequent protein–protein interactions. Recent work has provided strong support for the presence of a tertiary structure in the cytoplasmic face in rhodopsin in the dark state and its change upon light activation (8, 10–12, 15, 18, 23). Thus, systematic studies of single-cysteine substitution mutants and of double-cysteine mutants have established the proximity relationships between amino acids in different regions of the cytoplasmic face (refs 9, 10, and 14 and unpublished work of Cai et al., Klein-Seetharaman et al., and Altenbach et al.). Further, extensive EPR spectroscopy of spin-labeled cysteine mutants has demonstrated movements of helices within the TM domain (7–12). Additionally, a disulfide cross-link between a cysteine placed at position 139 and a second cysteine at positions 248–251 was found to block G<sub>T</sub> activation (9). Extending this observation, we have now studied the effects of six disulfide cross-links between different regions of the cytoplasmic face (Figure 1) on light activation of rhodopsin and its interactions with G<sub>T</sub> and RK.

None of the disulfide bonds affected the formation of  $\lambda_{380}$ -absorbing Meta II on illumination, a result in agreement with the previous finding of Sheikh et al. (13). Further, no effect on the specificity of retinal isomerization, namely, 11-*cis*-to-*all-trans*-retinal, was found. Careful analysis in every case of the retinal produced on light activation showed that *all-trans*-retinal was the essential product (data not shown). In previous studies, amino acid replacements were introduced in the retinal binding pocket of bacteriorhodopsin (24) and the corresponding bacteriorhodopsin mutants formed on reconstitution with *all-trans*-retinal were examined for specificity of isomerization on illumination. Significant formation of retinal isomers other than the normal 13-*cis*-retinal was found, an indication of the detectable loss of specificity in isomerization. It is interesting now to find that none of the restrictions placed on the conformational change in rhodopsin affects the formation of the Meta II or the specificity of retinal isomerization. However, significant differences were found in the decay rates of Meta II. The disulfide cross-linked mutants, A246C/Q312C, K245C/S338C, and H65C/316C, exhibited faster Meta II decay than normal. Interestingly, while the mutants with cross-links between the end of helix III (position 135 or 139) and the end of helix VI (position 248 or 250) exhibited no change in Meta II formation, both G<sub>T</sub> activation and phosphorylation by RK were abolished.

Figure 5 depicts the total profile of effects observed for the six disulfide cross-links. Overall, the changes in activities observed for the mutants in the reduced states (with DTT), relative to that of WT rhodopsin, can be ascribed to substitution of the two native amino acids in each case with cysteines. Here, the focus is on the distinctive effects observed in the different mutants in the cross-linked states (without DTT). There are three types of effects. Disulfide bond 1, between H65C and C316, positions that show a

change in distance on light activation by EPR spectroscopy (10), had little effect on either  $G_T$  activation or phosphorylation by RK. This result suggests that restriction of movement in this region of the tertiary structure is not critical for the recognition of the activated state by  $G_T$  or by RK. However, there is the possibility although remote that the disulfide bond was cleaved by exchange with a cysteine in the TM domain exposed after light activation. In contrast, both  $G_T$  activation and phosphorylation by RK were abolished by cross-links between the cytoplasmic ends of helices VI and VII (A246C/Q312C) and of helices III and VI (V139C/K248C, V139C/V250C, and R135C/V250C). The proximity between the cysteine pairs in these mutants in the dark and increases in distances between them upon illumination have been found previously (ref 9 and unpublished data of Cai et al.). The observed uniformly dramatic effects of the restrictions suggest that they prevent the conformational change in this region required for interaction of rhodopsin with both  $G_T$  and RK. There is, however, the alternative possibility that the disulfide bonds may simply cause steric hindrance to the approach of the two proteins. The third type of effect is shown by the cross-link between the cysteines in mutant K245C/S338C. The proximity between these two cysteines in the dark was also clearly demonstrated, and an increase in distance upon light activation was exhibited by both disulfide cross-linking and EPR studies (14). It is not surprising that phosphorylation was abolished by tethering the C-terminal tail of rhodopsin, which is the substrate component for RK to the loop region between helices V and VI. However, it is very interesting that this cross-link showed marked increases in the extent of  $G_T$  activation in comparison with the reduced form and with WT rhodopsin. Presumably, the specific conformation recognized by  $G_T$  was stabilized by this cross-link.

The results reported here have underscored the regions in the cytoplasmic face of rhodopsin that are required for the binding and activation of the two key proteins,  $G_T$  and RK. Further, the study has demonstrated that the conformational change in rhodopsin upon light activation need not be cooperative but can be segmental. This important conclusion was also supported by a previous EPR study of the constitutively active mutant E134Q (25).

#### ACKNOWLEDGMENT

We thank Professor U. L. RajBhandary of the Biology Department of the Massachusetts Institute of Technology and members of this laboratory for helpful discussions. Ms. Judy Carlin's assistance during the preparation of the manuscript is gratefully acknowledged.

#### REFERENCES

- Hwa, J., Reeves, P. J., Klein-Seetharaman, J., Davidson, F., and Khorana, H. G. (1999) *Proc. Natl. Acad. Sci. U.S.A.* 96, 1932–1935.
- König, B., Arendt, A., McDowell, J. H., Kahlert, M., Hargrave, P. A., and Hofmann, K. P. (1989) *Proc. Natl. Acad. Sci. U.S.A.* 86, 6878–6882.
- Franke, R. R., Sakmar, T. P., Graham, R. M., and Khorana, H. G. (1992) *J. Biol. Chem.* 267, 14767–14774.
- Palcewski, K., Buczyko, J., Kaplan, M. W., Polans, A. S., and Crabb, J. W. (1991) *J. Biol. Chem.* 266, 12949–12955.
- Shi, W., Osawa, S., Dickerson, C. D., and Weiss, E. R. (1995) *J. Biol. Chem.* 270, 2112–2119.
- Thurmond, R. L., Creuzenet, C., Reeves, P. J., and Khorana, H. G. (1997) *Proc. Natl. Acad. Sci. U.S.A.* 94, 1715–1720.
- Farahbakhsh, Z. T., Ridge, K. D., Khorana, H. G., and Hubbell, W. L. (1995) *Biochemistry* 34, 8812–8819.
- Altenbach, C., Yang, K., Farrens, D. L., Farahbakhsh, Z. T., Khorana, H. G., and Hubbell, W. L. (1996) *Biochemistry* 35, 12470–12478.
- Farrens, D. L., Altenbach, C., Yang, K., Hubbell, W. L., and Khorana, H. G. (1996) *Science* 274, 768–770.
- Yang, K., Farrens, D. L., Altenbach, C., Farahbakhsh, Z. T., Hubbell, W. L., and Khorana, H. G. (1996) *Biochemistry* 35, 14040–14046.
- Altenbach, C., Cai, K., Khorana, H. G., and Hubbell, W. L. (1999) *Biochemistry* 38, 7931–7937.
- Altenbach, C., Klein-Seetharaman, J., Hwa, J., Khorana, H. G., and Hubbell, W. L. (1999) *Biochemistry* 38, 7945–7949.
- Sheikh, S. P., Zvyaga, T. A., Cypess, A. M., Lichtarge, O., Sakamer, T. P., and Bourne, H. R. (1996) *Nature* 383, 347–350.
- Cai, K., Langen, R., Hubbell, W. L., and Khorana, H. G. (1997) *Proc. Natl. Acad. Sci. U.S.A.* 94, 14267–14272.
- Cai, K., Klein-Seetharaman, J., Farrens, D., Cheng, Z., Altenbach, C. A., Hubbell, W. L., and Khorana, H. G. (1999) *Biochemistry* 38, 7925–7930.
- Baehr, W., Morita, E. A., Swanson, R. J., and Applebury, M. L. (1982) *J. Biol. Chem.* 257, 6452–6460.
- Cha, K., Bruel, C., Inglese, J., and Khorana, H. G. (1997) *Proc. Natl. Acad. Sci. U.S.A.* 94, 10577–10582.
- Klein-Seetharaman, J., Hwa, J., Cai, K., Altenbach, C., Hubbell, W. L., and Khorana, H. G. (1999) *Biochemistry* 38, 7938–7944.
- Resek, J. F., Farahbakhsh, Z. T., Hubbell, W. L., and Khorana, H. G. (1993) *Biochemistry* 32, 12025–12031.
- Yang, K., Farrens, D. L., Hubbell, W. L., and Khorana, H. G. (1996) *Biochemistry* 35, 12464–12469.
- Ridge, K. D., Zhang, C., and Khorana, H. G. (1995) *Biochemistry* 34, 8804–8811.
- Scherrer, P., Mathew, M. K., Sperling, W., and Stoeckenius, W. (1989) *Biochemistry* 28, 829–834.
- Langen, R., Cai, K., Altenbach, C., Khorana, H. G., and Hubbell, W. L. (1999) *Biochemistry* (in press).
- Greenhalgh, D. A., Farrens, D. L., Subramaniam, S., and Khorana, H. G. (1993) *J. Biol. Chem.* 268, 20305–20311.
- Kim, J., Altenbach, C., Thurmond, R. L., Khorana, H. G., and Hubbell, W. L. (1997) *Proc. Natl. Acad. Sci. U.S.A.* 94, 14273–14278.

BI9912443